

Large-Eddy Simulation of Flow around Buildings: Validation and Sensitivity Analysis

T. Okaze¹, H. Kikumoto², H. Ono³, M. Imano⁴, N. Ikegaya⁵, T. Hasama⁶,
K. Nakao³, T. Kishida³, Y. Tabata⁷, R. Yoshie⁸ and Y. Tominaga⁹

¹School of Environment and Society
Tokyo Institute of Technology, Yokohama, Kanagawa 226-8502, Japan

²Institute of Industrial Science
The University of Tokyo, Meguro, Tokyo 153-8505, Japan

³Central Research Institute of Electric Power Industry, Abiko, Chiba 270-1194, Japan

⁴OCAEL Co. Ltd., Shibaura, Tokyo 108-0023, Japan

⁵Interdisciplinary Graduate School of Engineering Sciences
Kyushu University, Kasuga, Fukuoka 816-8580 Japan

⁶Technical Research Institute
Kajima Corporation, Chofu, Tokyo 182-0036 Japan

⁷Technical Research Institute
Obayashi Corporation, Kiyose, Tokyo 204-8558, Japan

⁸Tokyo Polytechnic University, Atsugi, Kanagawa 243-0297, Japan

⁹Department of Architecture and Building Engineering
Niigata Institute of Technology, Kashiwazaki, Niigata 945-1195, Japan

Abstract

Appropriate LES guidelines for the pedestrian wind environment in urban areas are being established by a working group from the Architectural Institute of Japan. In this study, large-eddy simulations were conducted for the flow field around an isolated building and within a cubic building array to clarify the influence of various computational conditions on turbulent statistics. First, a cross comparison study was performed by examining both experimental and large-eddy simulation (LES) results for various computational grid arrangements, sub-grid scale turbulence models, spatial derivation schemes (for the convection term), and convergence criterion for a coupling algorithm relating the flow and pressure fields in the flow field around an isolated building. Next, the appropriate computational conditions, obtained from the LES for flow around an isolated building, were applied to the LES for flow within a building array.

Introduction

Computational fluid dynamics (CFD) is widely used for predicting the urban wind environment. Several best practice guidelines have been proposed as verification and validation processes for CFD. A group called the European Cooperation in Science and Technology (COST) compiled a set of specific recommendations for the use of CFD based on a detailed review of the literature, and discussed the quality assurance of CFD results [1, 2]. A working group from the Architectural Institute of Japan (AIJ) conducted extensive cross comparisons between CFD simulation results and high-quality wind-tunnel experiments to develop guidelines [3, 4]. These guidelines focus on a steady-state simulation using the Reynolds-averaged Navier–Stokes equations (RANS) model. However, in recent years, increasing access to computing power has led to the prediction of flow fields using large-eddy simulation (LES). These LESs have mainly been conducted by experts in CFD using sophisticated

computational conditions, which yield good results with respect to effectively removing computational errors. The working group from AIJ is in the process of establishing appropriate LES guidelines for the pedestrian wind environment in a built-up area.

In the first part of this study, the working group from AIJ conducted LESs for a flow field around an isolated building. These LES results were compared with experimental results from a wind tunnel experiment conducted at Tokyo Polytechnic University [5] for validation purposes. Subsequently, a cross comparison study was performed by changing the computational grids, sub-grid scale (SGS) turbulence models, and spatial derivation schemes for the convection term.

In the latter part of this study, an outline of LESs for a flow field within a simple cubic building array is introduced. These computations were performed to validate and extend the appropriate computational conditions obtained from a LES of the flow around an isolated building to the conditions in a built-up environment. Furthermore, a building canopy model was applied to the surrounding buildings of the building array in order to reproduce the effect of the spatially-averaged drag force of the buildings. The reduction of the computational cost and the effect of simplifying the calculation procedure were both further investigated. The comparison of the results of the LES modeling flow within the building array and results of the wind tunnel experiment will be presented at the conference.

Inflow boundary condition

It is known that inflow turbulence properties greatly affect the flow field around buildings. Various inflow generating methods have been proposed based on recycling methods and synthetic methods, as reviewed in detail by Wu [6]. However, a method that can reproduce not only mean wind velocity and the turbulent statistics but also the instantaneous turbulent structures and the

power spectra of the target inflow has not been well established. Therefore, we performed a preliminary LES computation in which the approaching section of roughness blocks and spires in the wind tunnel were completely reproduced, as shown Figure 5. The preliminary simulation was performed using a high-performance computer with 32 nodes in parallel. Each node consists of 8×2 cores with a 2.6 GHz CPU and a 32 GB memory. To achieve high efficiency parallel computation, the WALE SGS turbulence model was used for the preliminary simulation. The instantaneous wind velocity was stored with a sampling interval of 1.0×10^{-3} s at the data storage plane, shown in Figure 1, which corresponds to the inflow boundary of the main simulation. Figure 2 shows the comparisons for the inflow turbulent statistics between the preliminary LES and the experimental results; the results obtained from preliminary LES corresponded well with the experimental results.

Flow around an isolated building

Calculation setup

The wind tunnel experiment conducted at Tokyo Polytechnic University [5] was used as the source of validation data for the LES. The computational domain was set to $12.5H(x) \times 6.0H(y) \times 5.0H(z)$, where H is the building height. An orthogonal grid system was applied. Three computational grids were used in this study: Grid10, Grid20, and Grid40. The building width was uniformly discretized into 10, 20, and 40 grids, which correspond to the grid names, respectively. The grid spacing was expanded at a distance from the building and the wind tunnel walls with an expansion ratio of 1.08 or less. The grid arrangement for Grid20 is illustrated in Figure 3.

The open source CFD code OpenFOAM v1606+ [7] was used for the LES. A fully implicit scheme was employed for the time integration. A second-order linear interpolation scheme was used for the diffusion term. Two types of spatial derivatives for the convection term were used in this study. First, the first-order upwind interpolation scheme was mixed with the second-order linear interpolation scheme with specific blending ratios: 0%, 5%, 10%, 20%, 40%, and 100%. Second, the first-order upwind scheme was automatically mixed with the second-order linear scheme at a blending ratio of 40% or less when the convection boundedness criterion was violated to avoid numerical oscillations. This scheme is implemented as ‘filteredLinear2’ in OpenFOAM [7]. The blending ratio in this scheme locally changes depending on the boundedness criterion of numerical oscillations. To store the time history of inflow turbulence, we performed a preliminary LES computation in which the approaching section of roughness blocks and spires in the wind tunnel were completely reproduced.

Test cases

Tests on thirteen cases were carried out; descriptions of the cases are listed in Table 1. Case-0 is the reference case with the standard Smagorinsky model ($C_s = 0.12$) as the SGS model, the linear interpolation scheme mixed with the upwind scheme automatically by 40% (implemented as “filteredLinear2V”) as the discretization of convection term, Grid20, and 1.0×10^{-7} as the convergence criterion for the Poisson equation of the correction of pressure in the PISO algorithm. To investigate the influence of the computational conditions on the predicted results, the computational conditions were changed step-by-step, and the results of each case were compared with the results of Case-0. For the Case-1 series, the effect of the computational grid is included. For the Case-2 series, the effect of the numerical dissipation caused by the first-order upwind scheme is shown. For the Case-3 series, the effect of the SGS turbulence model is investigated. For Case-4, the effect of the tolerance of the convergence criterion for the Poisson equation is discussed.

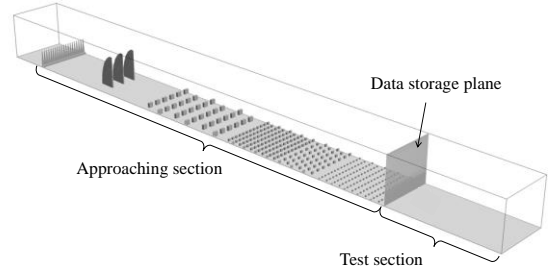


Figure 1. Schematic of a preliminary simulation

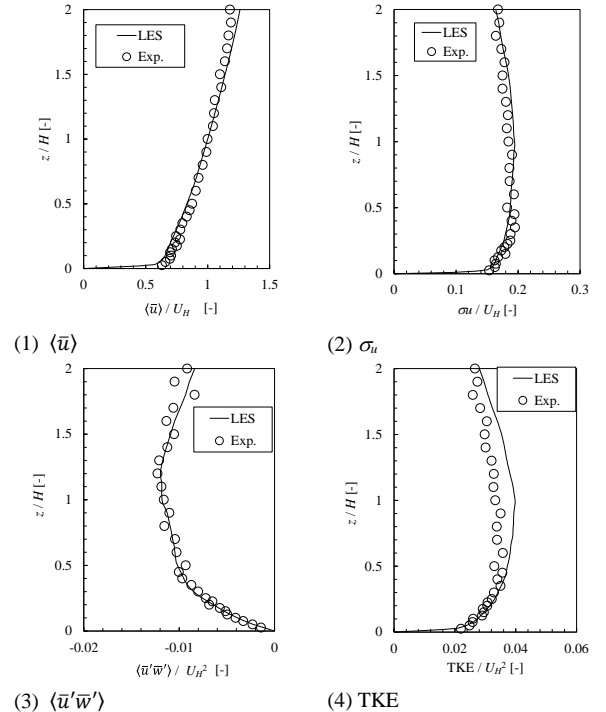


Figure 2. Turbulent statistics at inflow boundary

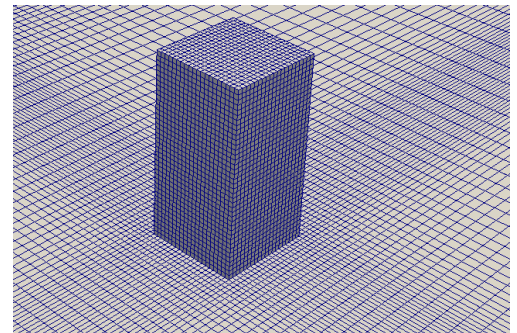


Figure 3. Grid arrangement around a building (Grid20)

Results and discussion

All the values in the experimental and LES results were normalized with the building height, H and the mean wind velocity at H at the inflow boundary, U_H . Table 2 presents the results of the evaluation of the agreement between the experimental and LES results by using a factor of 2 of observations (FAC2) [8]. FAC2 is evaluated as follows:

$$FAC2 = \frac{1}{N} \sum_{i=1}^N n_i \quad \text{with } n_i = \begin{cases} 1 & \text{for } 0.5 \leq \frac{P_i}{O_i} \leq 2 \\ 1 & \text{for } |O_i| \leq W \text{ and } |P_i| \leq W \\ 0 & \text{else} \end{cases}, \quad (1)$$

where N is the total number of measurement points, O is the observation result, and P is the predicted result. W was set to 0.05 in this study.

The values for Case-0 (Grid20) and Case-1-Grid40 were almost identical, but those for Case-1-Grid10 were somewhat poorer than those for Case 0 (Grid20). Figure 4 compares the vertical profiles of the streamwise component of mean velocity $\langle \bar{u} \rangle$ and the variance of the fluctuation of the streamwise component $\langle \bar{u}'^2 \rangle$ for Case 0 (Grid 20), Case-1-Grid10, and Case-1-Grid40 along five lines ($x = -0.75H, -0.25H, 0.25H, 0.75H,$ and $1.25H$) in the vertical plane at $y = 0H$. The results for Case-0 agreed well with the experimental results. There were no major changes between the results for Case-0 and Case-1-Grid40. The values for Case-1-Grid10 were slightly different from the experimental and the computational results for Case-0. The value of $\langle \bar{u}'^2 \rangle$ at the separation region near the building top for Case-1-Grid10 was underestimated, probably because of insufficient spatial resolution for reproducing the small-scale fluctuations in this region. These results indicate that the use of Grid20 is suitable for predicting the mean wind velocity and second order turbulent statistics around the building considered in this study.

For the Case-2 series that changed the blending ratio of the first-order upwind scheme to the second-order central scheme, FAC2 decreased as the blending ratio increased. In particular, the FAC2 of the vertical fluctuation decreased with an increase in the blending ratio. Case-2-linear0.95 (5% blending ratio) yielded almost the same FAC2 as Case-0. Case-2-linear also yielded almost the same result with Case-0 as well, but remarkable numerical oscillations occurred (not shown).

For the Case-3 series that compared the different SGS models, the differences between Case-0 and Case-3-Cs0.10, Case-3-Cs0.17, and Case-3-WALE were small. The result with Case-3-laminar (No turbulence model) was somewhat lower than that for Case-0. However, FAC2 for Case-3-laminar also yielded fairly good results. This is due to the effect of the numerical dissipation derived from using the filteredLinear2V as the discretization scheme for the convection term. The blending ratio of the first-order upwind scheme in the filteredLinear2V might have a large value. In fact, the numerical oscillations were mostly eliminated in Case-3-laminar.

For Case-4-tol1e-2, which changed the final residual for the Poisson equation from 1.0×10^{-7} (used for Case 0) to 1.0×10^{-2} , both the mean wind velocity and the turbulence statistics were comparable to those for Case-0 in this study. According to Kajishima and Taira [9], as one of the convergence criteria of the Poisson equation for the correction of pressure, the divergence of wind velocity should be several orders of magnitude smaller than

$|\mathbf{u}|/\Delta$, where $|\mathbf{u}|$ is the magnitude of wind velocity and Δ is grid size. In fact, the average of the divergence was four orders of magnitude smaller than $|\mathbf{u}|/\Delta$ in Case 4-tol1e-2.

Flow within a building array

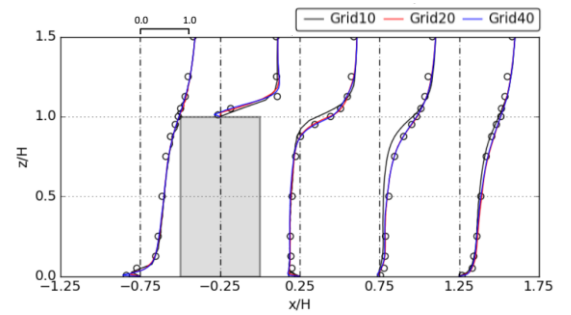
Calculation setup

LESs within a cubic building array are also being conducted. This section first investigated the applicability of appropriate computational conditions obtained from the LES of the flow around an isolated building to LESs modeling flow within building arrays. Subsequently, methods for accurately reproducing and simplifying the coverage of the surrounding building shapes are investigated. The canopy model [9, 10] was introduced to the surrounding buildings in order to decrease computational cost because it is not necessary to reproduce the surrounding buildings with high-resolution grids.

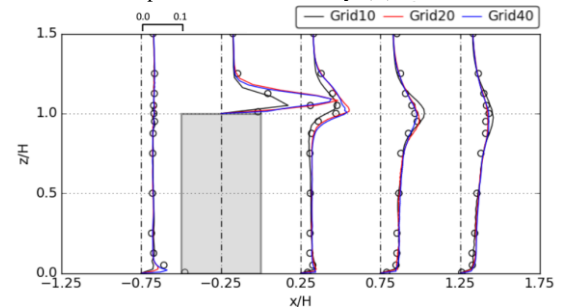
Figure 5 shows a schematic of the building array. The building array consisted of 81 cubic buildings built in nine rows and nine columns at intervals of H , where H is equal to the building height. The wind tunnel experiment within the building array was also conducted at Tokyo Polytech University. The wind velocity measurements were conducted around the three buildings in the center of the array, as shown in Figure 5. Figure 6 shows the grid arrangement used. The building width was uniformly discretized

Case	$\langle u \rangle$	$\langle v \rangle$	$\langle w \rangle$	$\langle u'^2 \rangle$	$\langle v'^2 \rangle$	$\langle w'^2 \rangle$	TKE
Case-0	0.94	0.93	0.86	0.97	0.91	0.84	0.98
Case-1-Grid10	0.86	0.95	0.79	0.93	0.88	0.81	0.93
Case-1-Grid40	0.93	0.92	0.87	0.99	0.90	0.84	1.00
Case-2-linear	0.93	0.93	0.86	0.94	0.88	0.83	0.96
Case-2-linear0.95	0.94	0.92	0.86	0.96	0.92	0.82	0.96
Case-2-linear0.90	0.92	0.93	0.85	0.91	0.93	0.76	0.92
Case-2-linear0.80	0.90	0.92	0.84	0.88	0.93	0.70	0.88
Case-2-linear0.60	0.85	0.91	0.78	0.82	0.88	0.56	0.84
Case-2-upwind	0.77	0.92	0.74	0.70	0.63	0.20	0.62
Case-3-Cs0.10	0.93	0.92	0.86	0.97	0.90	0.84	0.97
Case-3-Cs0.17	0.93	0.92	0.85	0.94	0.92	0.84	0.95
Case-3-WALE	0.93	0.92	0.87	0.95	0.89	0.85	0.97
Case-3-laminar	0.90	0.94	0.88	0.89	0.83	0.88	0.93
Case-4-tol1e-2	0.93	0.93	0.86	0.95	0.90	0.85	0.97

Table 2. Validation metric with FAC2



(1) Streamwise component of mean velocity $\langle \bar{u} \rangle / U_H$



(2) Variance of fluctuation of streamwise component $\langle \bar{u}'^2 \rangle / U_H^2$

Figure 4. Comparison of the vertical profiles of LES results with experimental result

Case	SGS model	Discretization of convection term	Grid	
Case-0	S model ($C_S = 0.12$)	filteredLinear2V	Grid20	
Case-1-Grid10	S model ($C_S = 0.12$)	filteredLinear2V	Grid10	
Case-1-Grid40			Grid40	
Case-2-linear		Central	Grid20	
Case-2-linear0.95		Central 95%+Upwind 5%		
Case-2-linear0.90		Central 90%+Upwind 10%		
Case-2-linear0.80		Central 80%+Upwind 20%		
Case-2-linear0.60		Central 60%+Upwind 4%		
Case-2-upwind		Upwind		
Case-3-Cs0.10	S model ($C_S = 0.10$)	filteredLinear2V	Grid20	
Case-3-Cs0.17	S model ($C_S = 0.17$)			
Case-3-WALE	WALE model			
Case-3-laminar	No turb. model			
Case-4-tol1e-2	S model ($C_S = 0.12$)			

Table 1. Test cases for LES around a building

into 20. With this grid, the evaluation region was also uniformly discretized. The total grid number used was 3.0×10^6 . Other computational conditions were chosen according to the results of the LES for the flow around the isolated building. These selected conditions were expected to yield good results with respect to the effective removal of computational errors.

Test cases

The influence of reproduction in the surrounding buildings was investigated. In the reference case, all cubic buildings were explicitly reproduced. Conversely, the test case applied a building canopy model [10, 11] to the surrounding district in the highlighted area seen in Figure 5 to reproduce the drag force created by the buildings. These computations will be completed, and the results will be presented at the conference with explicit attention given to how coverage of the shape of the surrounding buildings should be accurately reproduced.

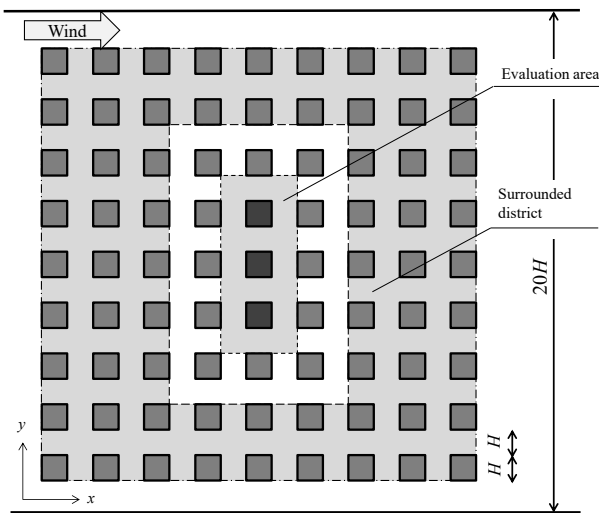


Figure 5. Schematic of building array

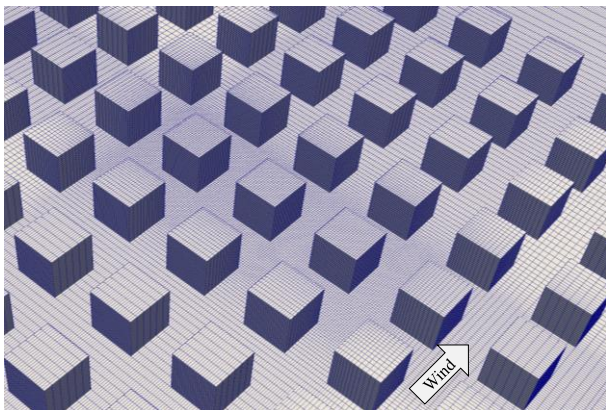


Figure 6. Grid arrangement for building array

Conclusions

The LESs for the flow around an isolated building rendered the following conclusions:

- The computational grid, in which the building width was discretized into 20 grids, provided enough resolution to reproduce the mean flow and turbulent statistics around the 1:1:2 shaped building model.
- For the discretization of the convection term, the linear interpolation scheme mixed with the upwind scheme automatically by 40% (implemented as “filteredLinear2V”),

and the linear interpolation scheme mixed with the 5% upwind scheme to yield good results.

- The difference in the results between cases using different SGS turbulence models was small.
- The convergence criterion for the Poisson equation of the correction of pressure in the PISO algorithm had little effect on the results of this study

Currently, LESs for the flow within a cubic building array are being conducted. We will confirm that the appropriate computational conditions obtained from the LES of flow around the isolated building may be applied to the LES for flow within the building array.

Acknowledgments

This research was supported by the joint research project of the Wind Engineering Joint Usage / Research Center, Tokyo Polytechnic University.

References

- [1] Franke J., Hellsten A., Schatzmann M. & Bertrand C., *Best practice guideline for the CFD simulation of flows in the urban environment*, COST Office Brussels, 2007.
- [2] Franke J., Hellsten A., Schlunzen K.H. & Carissimo B., The COST 732 Best Practice Guideline for CFD simulation of flows in the urban environment: a summary, *Int. J. Environ. Pollut.*, **44**, 2011, 419-427.
- [3] Tominaga Y., Mochida A., Yoshie R., Kataoka H., Nozu T., Yoshikawa M. & Shirasawa T., AIJ guidelines for practical applications of CFD to pedestrian wind environment around buildings, *J. Wind Eng. Ind. Aerodyn.*, **96**, 2008, 1749-1761.
- [4] Architectural Institute of Japan, *AIJ Benchmarks for Validation of CFD Simulations Applied to Pedestrian Wind Environment around Buildings*, Architectural Institute of Japan, 2016.
- [5] Tokyo Polytech University, *Database on Outdoor Air Pollution*, http://www.wind.arch.t-kougei.ac.jp/info_center/pollution/pollution.html.
- [6] Wu X., Inflow Turbulence Generation Methods. *Annu. Rev. Fluid Mech.*, **49**, 2017, 23-49.
- [7] OpenCFD Ltd (ESI Group), *OpenFOAM User Guide 2016*, <http://www.openfoam.com/>.
- [8] Schatzmann M., Olesen H. & Franke J., *COST 732 model evaluation case studies: approach and results*, COST Action; 2010.
- [9] Kajishima T. & Taira K., *Computational Fluid Dynamics*, Springer International Publishing, 2017, 95-96.
- [10] Maruyama T., Optimization of roughness parameters for staggered arrayed cubic blocks using experimental data, *J. Wind Eng. Ind. Aerodyn.*, **46-47**, 1993, 165-171.
- [11] Konno N., Ono A., Mochida A., Maruyama T., Hagishima A., Tanimoto J. & Tabata Y., Canopy flow modelling for reproducing aerodynamic effects of roughness arrays with various densities and configurations, *Proceedings of 13th International Conference on Wind Engineering*, 2011.